RSC Advances

PAPER

View Article Online
View Journal | View Issue

Cite this: *RSC Adv.*, 2020, **10**, 40148

Enhancing the mechanical and tribological properties of epoxy composites *via* incorporation of reactive bio-based epoxy functionalized graphene oxide†

Hao Wu,[abc] Chengbao Liu,[a] Li Cheng,[a] Yue Yu,[ab] Haichao Zhao *[a] and Liping Wang*[a]

The high rigidity and brittleness of traditional thermosetting resin based on bisphenol epoxy limits its many potential technical applications. Here, a novel tertiary amine containing cardanol-based epoxy resin (NC-514-DEA) was synthesized by reaction of diethanolamine (DEA) with cardanol epoxy resin (NC-514). Moreover, NC-514-DEA modified graphene oxide (GOND) was prepared and used as a reactive nano-reinforcing filler for epoxy composites. The results show that, compared with neat epoxy resin, the fracture toughness of the epoxy composite with 0.5 wt% GOND is increased by nearly 10%, and the friction coefficient is reduced from 0.567 to 0.408, demonstrating the best performance among specimens. The improved mechanical and wear resistance properties of prepared composites were attribute to the synergistic effect of NC-514-DEA and GO, which inhibited the generation and propagation of cracks by enhancing the interfacial interaction and distributing stress. In addition, the synthetic process of GOND is green, simple and efficient, providing a novel way for designing epoxy composite materials with many potential applications.

Received 10th September 2020
Accepted 23rd October 2020

DOI: 10.1039/d0ra07751h

rsc.li/rsc-advances

1. Introduction

Structural composite materials based on thermosetting epoxy resin has been widely applied in the fields of adhesives,[1] electronic packaging[2] and coatings[3] due to their excellent mechanical properties, fine processability and good heat resistance. However, the reaction between epoxy resin and curing agent tends to form a highly cross-linked network structure, resulting in the cured resin exhibiting greater rigidity, brittleness and lower interface interaction, which limits their usefulness in high-performance service environments.[4–6] Generally, the incorporation of high-quality nano-fillers, such as clay,[7] carbon fiber[8] and graphene[9] into the resin matrix is a convenient and effective way to improve the comprehensive performance of epoxy composites.

Graphene has been used to improve the strength,[10] toughness[11] and wear resistance[12] of epoxy composites since its inception. Nevertheless, the van der Waals force of the graphene sheets causes the G sheets to agglomerate. Therefore, EP/G nanocomposites cannot meet the requirements of practical applications.[9,13–15] Besides, due to the scarcity of reactive sites in graphene surface, it is difficult to modify graphene directly. As an important derivative, graphene oxide (GO) possesses abundant oxygen-containing groups, which provide the possibility for its multiple functionalization.[16] For example, Xia *et al.* use KH-560 to modify GO under thermal polymerization conditions to improve the anti-corrosion performance of epoxy nanocomposites.[17] Besides, the effect of GO functionalized with epoxy chains (diglycidyl ether of bisphenol A) on the mechanical properties of epoxy nanocomposites was studied by Wan *et al.*[18] In addition, Zhao *et al.* used dehydrated ethylenediamine modified GO to increase the tribological properties of epoxy composites.[4] The above studies have shown that functionalized GO can promote the dispersion of GO in epoxy matrix to a certain extent, and have a positive effect on improving the mechanical properties of epoxy composites. However, these reported modification processes are usually accompanied with the use of organic solvents, and complicated chemical treatment, during the modification process.[18,19] Considering the cost and sustainability of epoxy resin as a general structural material, the use of renewable resources to modify GO for improving

[a]*Key Laboratory of Marine Materials and Related Technologies, Zhejiang Key Laboratory of Marine Materials and Protective Technologies, Ningbo Institute of Materials Technology and Engineering, Chinese Academy of Sciences, Ningbo 315201, China. E-mail: zhaohaichao@nimte.ac.cn; wangliping@nimte.ac.cn*

[b]*Nano Science and Technology Institute, University of Science and Technology of China, Suzhou, 215123, China*

[c]*Innovation Academy of South China Sea Ecology and Environmental Engineering, Chinese Academy of Sciences, Guangzhou 510301, China*

† Electronic supplementary information (ESI) available. See DOI: 10.1039/d0ra07751h

the comprehensive mechanical properties and wear resistance of epoxy nanocomposites has great engineering significance.

In recent years, bio-based materials have received widespread attention because of reducing our excessive dependence on fossil resources and meeting the needs of green developments.[20] Cardanol epoxy resin is one of the important derivatives of natural product cashew nut shell liquid. Especially, it has the advantages of low preparation cost, environmental protection and degradability,[21,22] and has been developed for the application of green flame retardant[23] and biological crosslinking agents[24] for epoxy resins. Therefore, it is necessary to design high performance epoxy nanocomposites by using of cashew phenol epoxy functionalized GO.

In this work, we synthesized a novel cardanol-based modified graphene oxide (GOND) through the electrostatic interaction between tertiary amine derived from cardanol-based epoxy resin and graphene oxide. The mechanical and wear resistance of EP/GOND epoxy nanocomposites were also investigated. The cardanol-based epoxy on GOND participates in the chemical bonding of the epoxy matrix network cross-linking process, increasing the interface interaction between GO and epoxy matrix. And this strong interface interaction promotes the force transfer between the filler and the epoxy matrix, which prevents the stress concentration and crack expansion. Therefore, the prepared composite material possessed superior mechanical and wear resistance, exhibiting potential for practical application.

2. Experimental

2.1. Materials

Graphene oxide was purchased from Suzhou Carbon Technology Co., Ltd. Diethanolamine (DEA) was purchased from Aladdin Industrial Corporation. And bisphenol F 861 epoxy was purchased from Wanhua Chemical Group Co., Ltd. NC-514 (cardanol epoxy resin) and lite-2002 curing agent were provided by Cardolite Corporation.

2.2. Synthesis of NC-514-DEA and functionalization of GO

Fig. 1a shows the synthesis schematic of cardanol-based epoxy resin with tertiary amine (NC-514). NC-514 and DEA are poured into the flask according to the mass ratio of 1 : 1, then heated at 60 degrees for 30 minutes. Meanwhile, 10 mg of graphene oxide powder was dispersed in 10 mL of deionized water and sonicated for 30 min to obtain a 1 mg mL^{-1} of GO aqueous dispersion. Finally, NC-514-DEA was added to the aqueous dispersion of graphene oxide and continue to stir rapidly, the reaction mechanism of action is shown the in Fig. 1b. Then the solid mixture was purified by washing with ethanol solvent, and centrifugation (6000 rpm, 5 min). Finally, the ethanol slurry containing NC-514-DEA grafted GO was obtained.

2.3. Fabrication of epoxy composites

A typical procedure for preparation of epoxy composite with 0.5% modified GO ($GOND_{0.5\%}$) is as follows. The determined GOND slurry was added to the bisphenol F epoxy resin (3 g) in a given amount (0.5%), and stirred quickly for a period of time, then the lite-2002 curing agent (1.8 g) was added and stirred for a certain time. After removing the bubbles by the vacuum, the mixture was poured into a preheated polytetrafluoroethylene mold a 3 cm × 3 cm × 2 mm Q235 steel plate cured in an oven at 60 °C for 12 hours. For comparison, the composites without and with 0.1%, 0.25% and 1% (named EP, $GOND_{0.1\%}$, $GOND_{0.25\%}$, $GOND_{1\%}$) was prepared in the same procedure.

2.4. Characterization

The structural properties of GO and GOND were characterized by Fourier transform infrared spectroscopy (FTIR, NICOLET 6700) and a Raman spectroscopy (Renishaw in Via Reflex),their chemical composition and surface morphology were characterized by X-ray photoelectron spectroscopy (XPS, AXIS ULTRA DLD), transmission electron microscope (TEM, JEOL2100) and scanning probe microscope (SPM, Dimension 3100). The ^1H

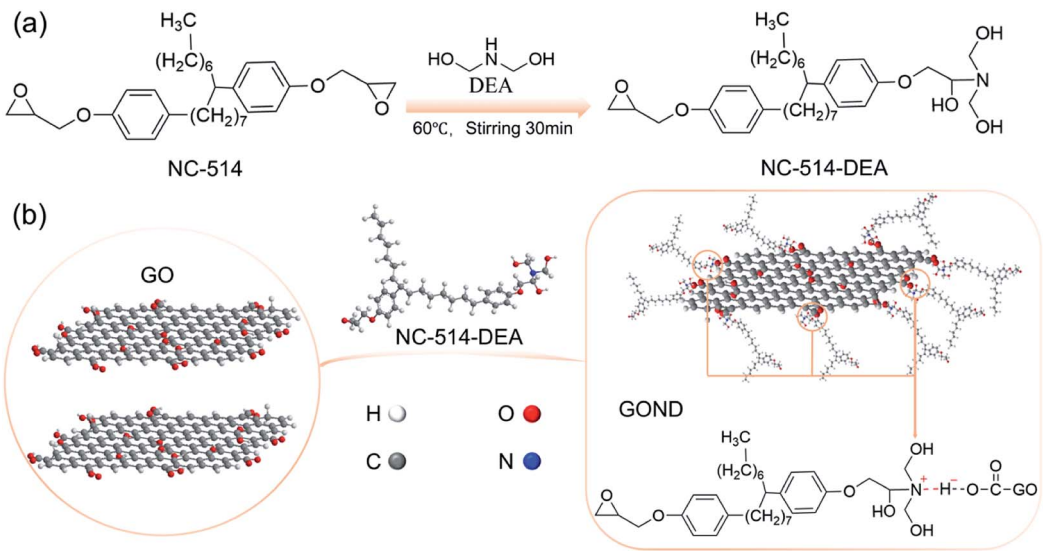

Fig. 1 Schematic presentation of the preparation of (a) NC-514-DEA and (b) GOND.

NMR spectra of NC-514 and NC-514-DEA were measured on Nuclear Magnetic Resonance Spectrometer (NMR, AVANCE III 400 MHz) with $CDCl_3$ as the solvent. The composite materials were analyzed with a dynamic mechanical (DMA) analyzer in the range of 1 HZ, −30–180 °C dynamic mechanical thermal analysis performance at a constant heating rate of 5 °C min^{-1}, and the thermal stability of graphene oxide epoxy composites was studied with thermogravimetrc (TGA) at a rate of 10 °C min^{-1} under a nitrogen atmosphere at a rate of 200 mL min^{-1}. The tensile strength and elongation of graphene oxide epoxy resin composites are based on the stress–strain curve obtained from a desktop electronic universal testing machine (crosshead speed 2 mm min^{-1}). Then the field emission scanning electron microscope thermal field (SEM, FEI Quanta FEG 250) was used to observe the cross-section morphology after breaking.

2.5. Friction tests

The tribological performance of the composite coatings under dry conditions is performed on a UMT-3 friction meter (Bruker-CETR, USA) with a constant load of 2 N, 3 Hz sliding frequency for 1800 seconds and a length of 5 mm. The 316 steel ball with a diameter of 3 mm was used as the friction pair. The friction mode is reciprocating friction. Observe the morphology of wear scars and debris with SEM, besides using laser confocal microscope (VK-X200K) to observe the wear depth and wear trajectory of the coating. Each sample was rubbed three times. The wear rate of the coating can be calculated using the depth of wear according to the formula given in the literature.[25]

$$W = V/F \times L$$

V in the formula refers to the volume of the coating wear, F is the normal load applied to the surface of the coating, and L is the length of the coating wear scar.

3. Results and discussion

3.1. Structural characterization and mechanical properties

^{1}H NMR spectra was used to determine the chemical structure of NC-514-DEA. As shown in Fig. S1,† the characteristic peaks of epoxy NC-514 were located at 2.7 ppm and 2.5 ppm.[26] After reacting with DEA, NC-514-DEA has the typical peak of NC-514, and its intensity at the characteristic peak of the epoxy group decreases, illustrating the successful preparation of NC-514-DEA. The FTIR spectrum is used to explain the mechanism of the interaction between cardanol epoxy and GO (Fig. 2a). For epoxy containing cardanol (NC-514), 2926 and 2855 cm^{-1} are

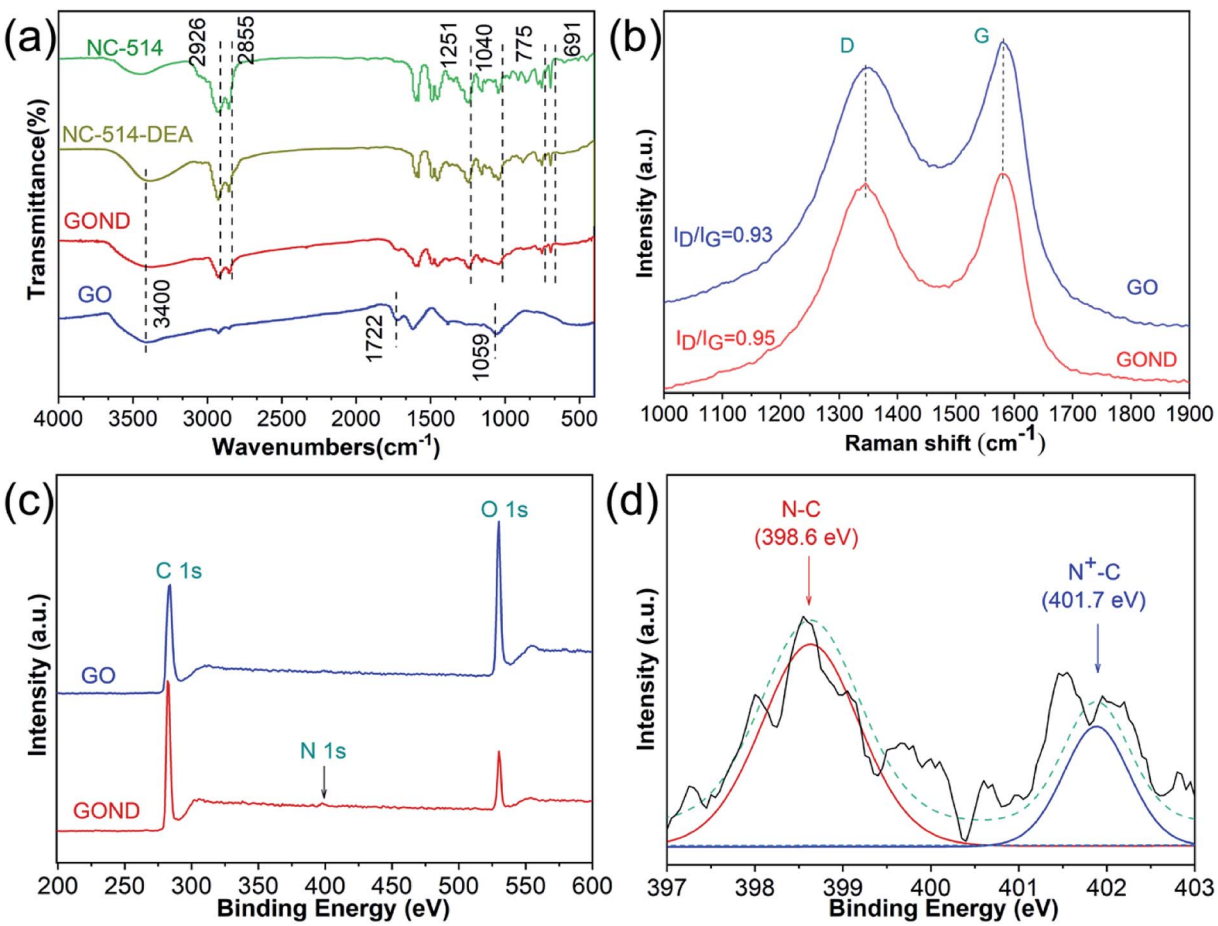

Fig. 2 (a) FTIR spectra of GO, NC-514, NC-514-DEA and GOND; and (b) Raman spectra of GO and GOND; XPS spectra of (c) GO and GOND, (d) N 1s spectra of GOND.

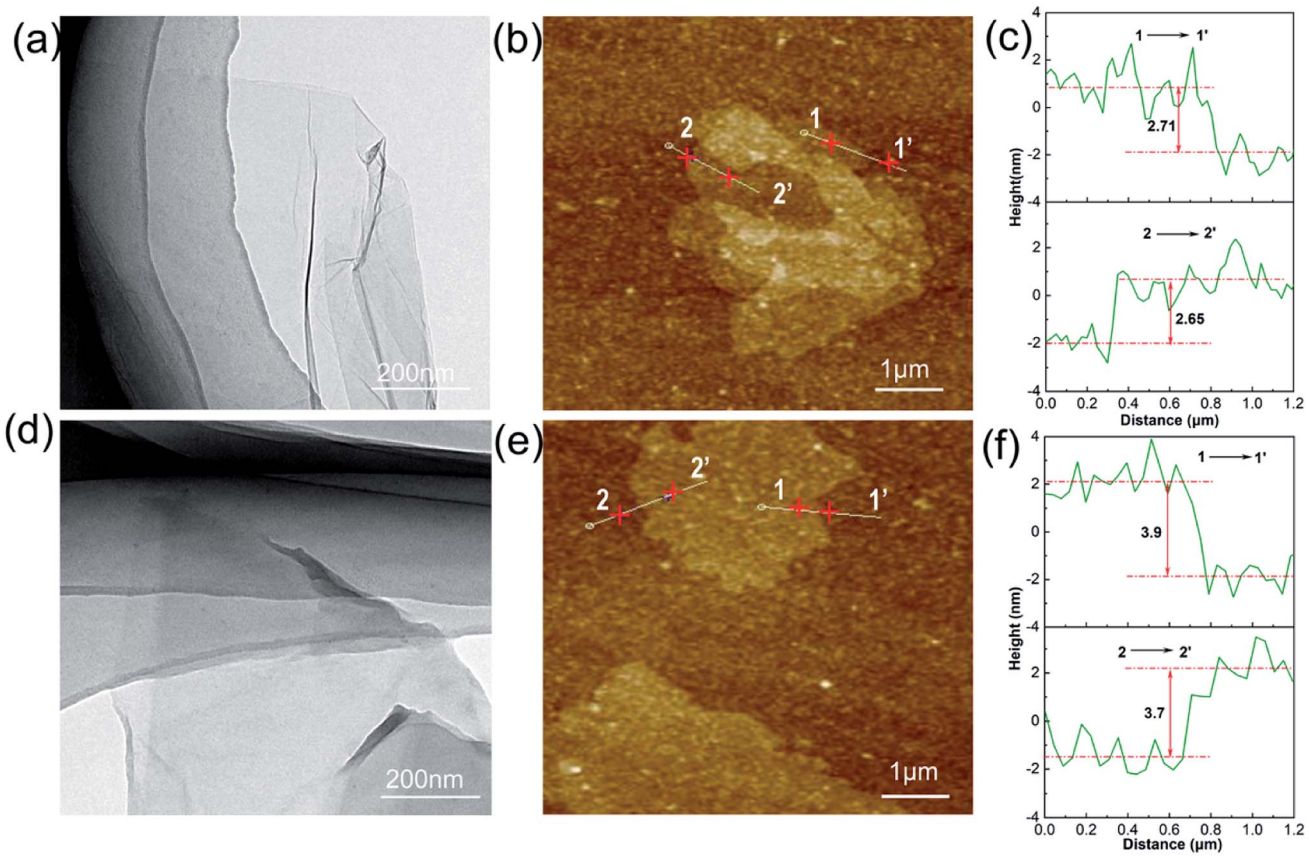

Fig. 3 TEM and SPM images of (a–c) GO and (d–f) GOND after dispersion in ethanol, respectively.

the absorption bands of C–C and C–H, respectively. and the bands at 1251 and 1040 cm^{-1} are the stretching of the C–O–C, in addition 1–3 substituted benzene in cardanol stretching 775 and 691 cm^{-1}.[21,27] After reaction with DEA, the strong O–H absorption band at 3400 cm^{-1} appeared, and the intensity of the epoxy absorption band decreased, indicating the presence of ring opening reaction between DEA and cardanol epoxy monomer. For GO, three characteristic absorption bands at 3400, 1722 and 1059 cm^{-1} are the stretching of O–H, C=C and C–O–C.[3,25] In the absorption spectrum of GOND, GOND exhibits both the characteristic absorptions from GO and NC-514-DEA, indicating that the GOND surface is successfully grafted by NC-514-DEA. The disorder level of GO is often expressed by the intensity ratio of the D band to the G band of Raman (I_D/I_G).[28,29] Fig. 2b shows that the intensity of I_D/I_G of GO grafted with NC-514-DEA increased from 0.93 to 0.95. Obviously, NC-514-DEA on the surface of GO increases the disorder level of GO. This illustrates the successful grafting reaction of GO and NC-514-DEA. Fig. 2c and d show the results of XPS analysis of GO and GOND composition and chemical state measurement. With the access of NC-514-DEA on the GO surface (Fig. 2c), a weak N atom peak appeared in GOND. In addition, the results in Fig. 2d show that the electron transfer between the acid and base of GO and NC-514-DEA forms a proton amine ($–COO^-N^+R_3$), which in turn forms a more stable complex. It is precisely because of this strong bond that 401.7 eV appears in the core level spectrum of N 1s.[30,31]

TEM and SPM can observe the surface morphological changes of GO and GOND, as shown in Fig. 3. It can be seen from Fig. 3a microstructure of GO shows the surface of GO is a single layer of smooth structure. And the GOND TEM image (Fig. 3d) has a reduced transparency, which is attributed to the introduction of NC-514-DEA.[3,32] From the results of SPM, the modified graphene oxide still has a two-dimensional sheet structure in Fig. 3b and e. The difference is that the thickness of the lamella increased from 2.7 nm to 3.7 nm, as is shown in Fig. 3c and f, which indicates that the cardanol epoxy was successfully grafted on the surface of GO. The interfacial compatibility of epoxy and nanofiller was analyzed by Raman scan, as shown in Fig. S2,† the change of $EP/GO_{0.5\%}$ strength (I_{epoxy}/I_{GO}) is more obvious, while the change of $EP/GOND_{0.5\%}$ strength is not obvious, indicating that NC-514-DEA improves the epoxy dispersion of graphene oxide in epoxy resin.

DMA results revealed that the storage modulus of EP/GO is not significantly different from pure EP, and the composites with modified GO shows a higher storage modulus in the temperature range from −30 to 36 °C. The significant increase in storage modulus is due to strong interface interaction between epoxy matrix and the nanofiller GOND.[33] However, too much GOND will still accumulate, resulting in lower storage modulus in Fig. 4a. The temperature corresponding to the peak loss factor is the glass transition temperature (T_g) of the epoxy composite. Fig. 4b shows that the epoxy nanocomposite with GOND has a lower T_g

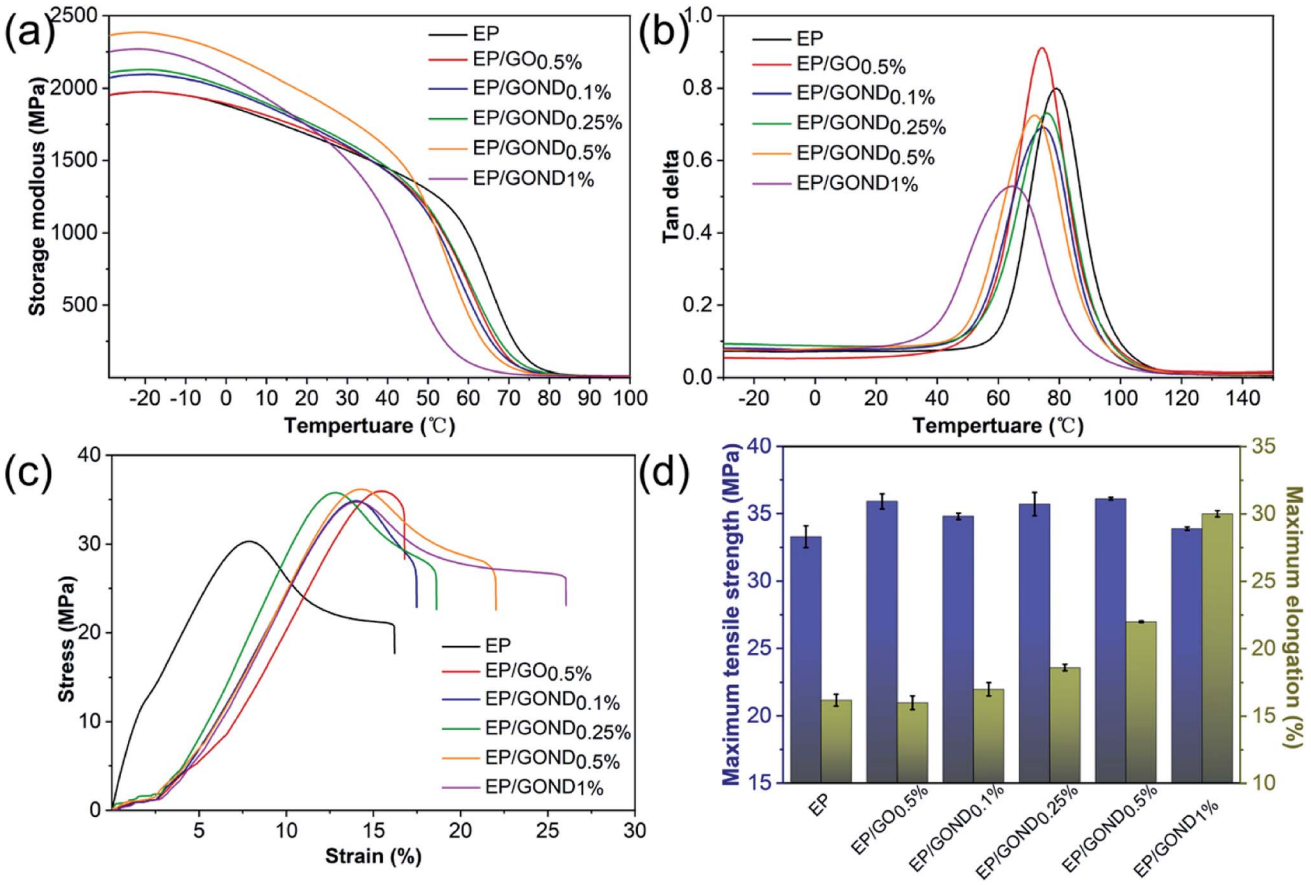

Fig. 4 Dynamic mechanical properties of EP and its nanocomposites (a) and (b); stress–strain curve of EP and its nanocomposites (c) and maximum tensile strength and maximum elongation (d).

compared to pure epoxy. This may be due to the well-dispersed GOND nanosheets change the cross-linked grid structure of the epoxy composites, which can increase the mutual transfer efficiency of force when the composite material moves, leading to the realization of the high elasticity of the composite material in advance. TGA is usually used to characterize the thermal stability of epoxy composites. As shown in Fig. S3,† there are no significant differences between the samples. When the heat loss of the composite material is 5%, the T5% of EP/$GOND_{0.5\%}$ increases by 20 °C. The existence of the sheet increases the heat capacity and interface interaction of the epoxy composite material, and hinders the degradation and volatilization of the material. This is attributed to the chemical bond between the GOND board and the epoxy matrix network skeleton, which is manifested in the improved thermal stability of the composite material.[34]

Fig. 4 shows the stress–strain curve of the nanocomposite tensile test and its maximum tensile strength and elongation at break at room temperature. The stress–strain curve shows that the tensile strength and elongation at break of adding GO or GOND have been improved (Fig. 4c). And the Fig. 4d shows that compared with pure epoxy resin, the addition of 0.5% GOND increases the fracture elongation of the nanocomposite from 16% to 22%, while the elongation at break with the addition of $GO_{0.5}$ hardly changes. For the 33 MPa maximum tensile strength of EP composite material, EP/$GOND_{0.5\%}$ increased the tensile strength to 36 MPa. Although adding 1% GOND can make the composite material a longer creep period, it reduces the tensile strength of the nanocomposite material. The friction between the epoxy matrix interface and the main cause of interface damage during sliding.

3.2. Microstructure of the epoxy composites

The fracture surface of different composites was presented in Fig. 5. It can be seen from (Fig. 5a) that the cross-section of pure epoxy resin is very smooth, which is a typical brittle fracture.[35] The agglomerated GO forms a bridging structure that is easily broken and deformed in the epoxy matrix (Fig. 5b), so a crack is formed between the interface and these structures. The modified GO has no obvious agglomeration (Fig. 5e), thus it can effectively transfer the energy generated by friction and slip between the filler and the matrix interface, and prevent the rapid expansion of cracks.[5,36] The 1% section of the filler is a tough fracture with many concave structures in Fig. 5f, indicating that the efficient energy transfer between the epoxy body and the filler, resulting in better toughness.[37] However, more fillers hinder the cross-linking efficiency of epoxy and reduce the strength of the composite. The above results illustrated that the GOND sheet not only increases the interface effect of the composite material and hinders the generation and

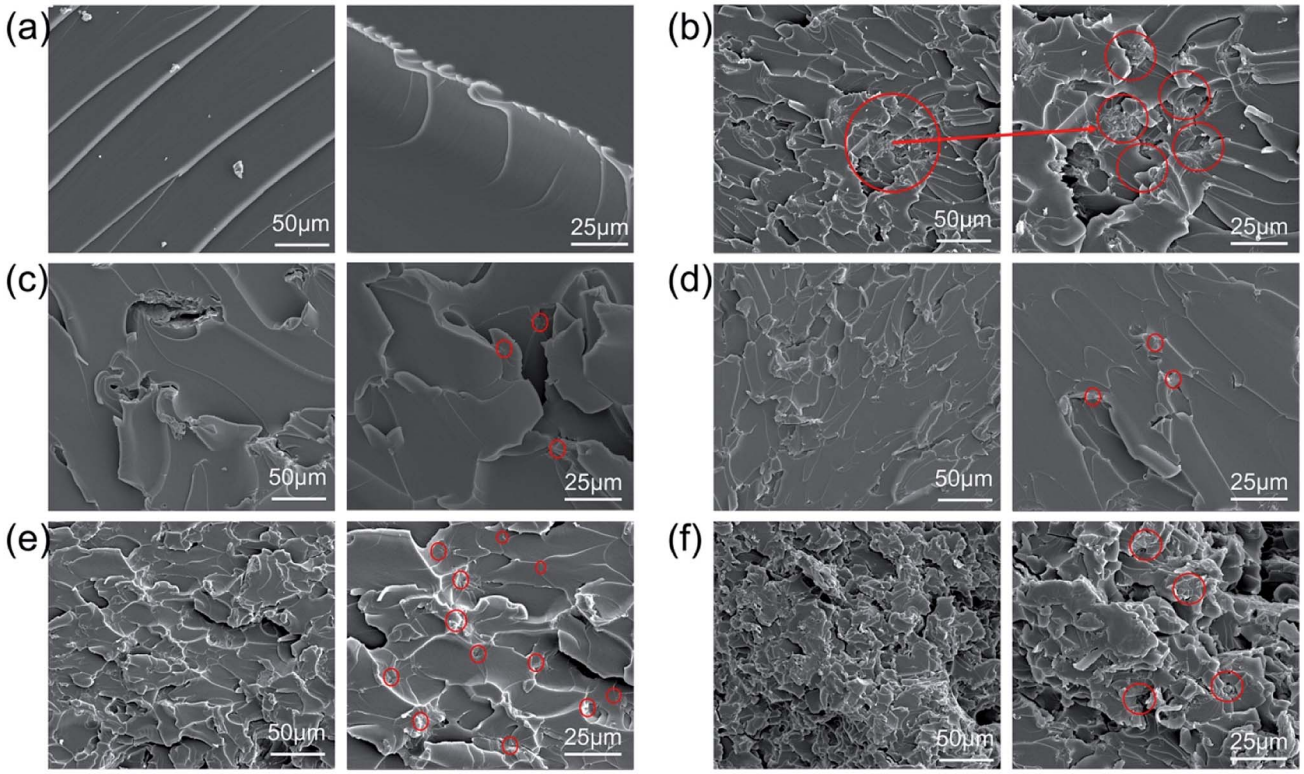

Fig. 5 Fracture surfaces of (a) EP, (b) EP/$GO_{0.5\%}$, (c) EP/$GOND_{0.1\%}$, (d) EP/$GOND_{0.25\%}$, (e) EP/$GOND_{0.5\%}$ and (f) EP/$GOND_{1\%}$.

expansion of cracks, but has a positive effect on the sliding between the well-dispersed GOND sheets.

3.3. Tribological characterization of epoxy composites

The Fig. 6 shows the friction coefficient and wear rate of the nanocomposite coating and pure EP. The friction coefficient of the composite coating with GO added is not significantly different from that of pure EP (Fig. 6a). The average friction coefficient of GO is reduced from 0.567 to 0.549, the friction coefficient of the composite coating with GOND (the content is 0.1%, 0.25%, 0.5%) is significantly better than pure EP, and the average friction coefficient of $GOND_{0.5\%}$ is reduced to 0.408. This proves that the synergistic effect of cardanol epoxy monomer and GO can improve the friction performance of the composite coating. However, when the amount of GOND added is 1%, the friction coefficient increases sharply or even higher than that of pure EP. This may be that too much GO causes agglomeration and affects the synergy between cardanol epoxy monomer and GO. Moreover, Fig. 6b shows the wear rate of the

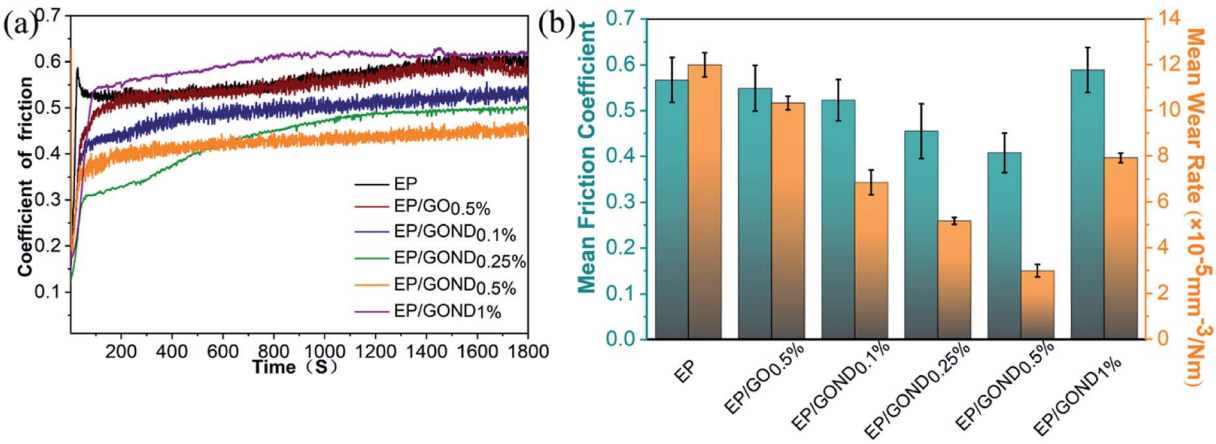

Fig. 6 Tribological properties of EP, EP/$GO_{0.5\%}$, EP/$GOND_{0.1\%}$, EP/$GOND_{0.25\%}$, EP/$GOND_{0.5\%}$ and EP/$GOND_{1\%}$ fraction lubricated at frequency 3 Hz under 2 N load at ambient environment. (a) COF; (b) mean COF and wear rate.

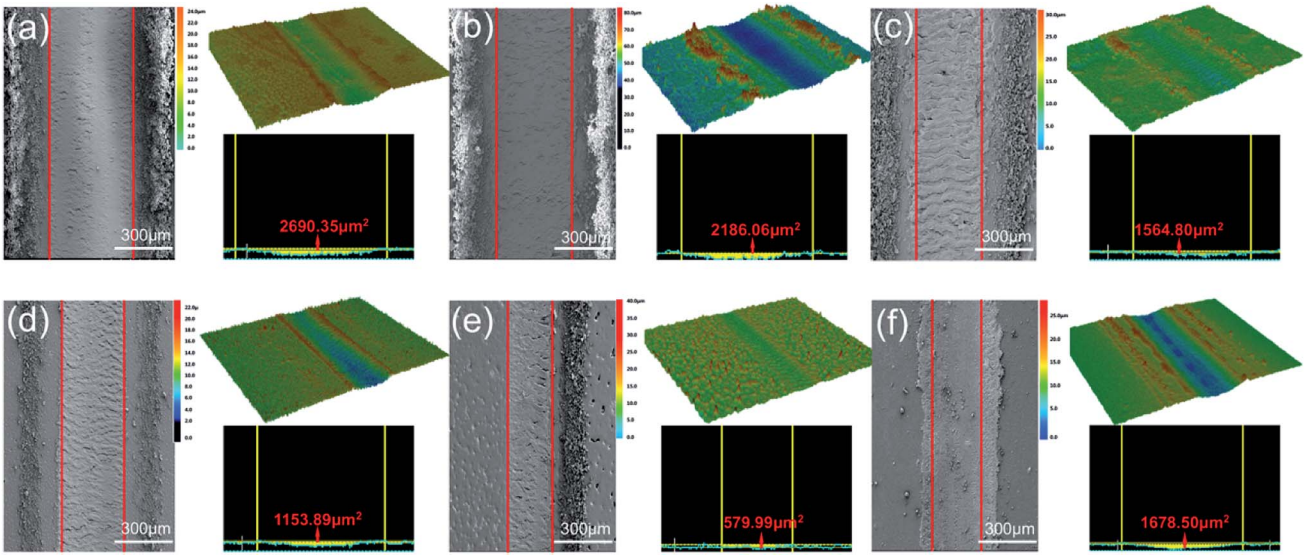

Fig. 7 SEM of wear tracks on composite coatings, and photos of wear scar profile and cross-sectional area at frequency 3 Hz under 2 N load at ambient environment with (a) EP, (b) EP/$GO_{0.5\%}$, (c) EP/$GOND_{0.1\%}$, (d) EP/$GOND_{0.25\%}$, (e) EP/$GOND_{0.5\%}$ and (f) EP/$GOND_{1\%}$.

composite coating and the average friction coefficient of the composite coating. The composite coatings with nanofillers all have lower wear rates. Compared with the addition of 0.5% GO, the average wear rate of the composite coating containing 0.5% GOND is reduced by about 71%, which is about 75% lower than the average wear rate of pure EP.

In order to better analyze the friction and wear mechanism, the morphology of wear scars and debris was observed with SEM, and the 3D surface profiler images and cross-sectional profile image of the composite coating after friction were observed with laser confocal in Fig. 7. Compared with pure EP, the addition of pure GO has no obvious change (Fig. 7b), while the composite coating with GOND (Fig. 7c–e) can effectively reduce the width of wear scars and the depth of wear. Among them, the wear scar with 0.5% GOND is the narrowest and the wear is lightest. With a 1% increase in wear scar width, the depth of wear is still effectively improved in Fig. 7f. These results indicate that, by adding GOND, the tribological properties of the composite coating can be increased. Fig. 7 and S4† show that the wear surface of the non-wear-resistant pure EP coating has delamination and cracks, and is relatively rough. The wear debris is shown as a massive block structure, which is the typical wear mechanism of thermosetting resin.[38] With the addition of fillers (go and GOND), there are fewer delamination and crack on the worn surface, and the size of the abrasive debris decreases, and the surface begins to become smoother. Obviously, GO with excellent friction properties can improve the tribological properties of the composite coating. Compared with epoxy composites with $GO_{0.5\%}$ wt sheet, composites containing $GOND_{0.5\%}$ has the narrowest wear marks and shallowest wear marks (Fig. 7e and S4e†), indicating that go and cardanol epoxy can improve the tribological properties of composite materials.

3.4. Friction and wear mechanism of epoxy composites

The wear mechanism of the composite coating is mainly divided into two stages: adhesive wear and fatigue wear.[38,39] For the EP coating he final wear scar SEM image has many long, wide and deep cracks in Fig. S5a.† At the beginning of the friction stage, due

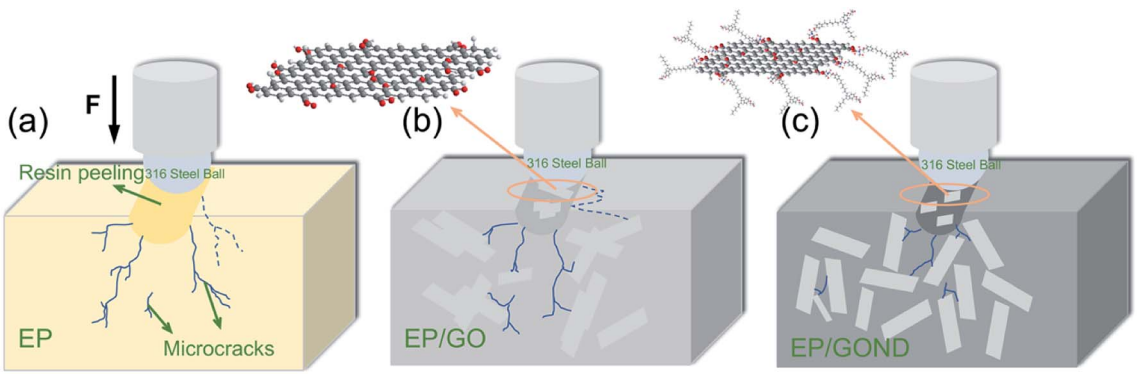

Fig. 8 Mechanism scheme for the wear behavior of composite coating without (a) EP, (b) EP/GO and (c) EP/GOND composite coating.

to the weak interface bonding force between the pure EP epoxy groups in the Fig. 8a, the generation and expansion of cracks can proceed quickly, and the coating peels off quickly, which results in low wear resistance and high wear rate.

For the composite coating with GO added, so the cracks are characterized by long and thin in Fig. S5b† the filler can hinder the propagation of cracks in the initial stage, and timely transfer the heat generated at the interface during the friction process[36,40] (Fig. 8b). As shown in Fig. S5,† adding GOND to the composite coating can improve the initiation and expansion of cracks during friction. In particular, when the added amount is 0.1 wt%, the cracks still have the characteristics of long and deep, which means that when the added amount is small, the crack suppression effect is not obvious (Fig. S5c†). It is worth noting that with the increase in the amount of addition, the initiation of cracks is effectively controlled, and the EP/GOND$_{0.5\%}$ coating has fewer cracks and the narrowest wear scar (Fig. S5e†). However, there are almost no obvious cracks in the composite coating with 1 wt% addition in the Fig. S5f.† Therefore, for composite coatings added with GOND in Fig. 8c, due to the excellent dispersion of graphene oxide with high lubricity and high specific surface area in the epoxy matrix, the epoxy matrix has high hardness and interface binding force, and high hardness can prevent the penetration depth of friction. The high interface binding force can better hinder crack propagation during friction, and the long cardanol chain gives the composite coating better toughness, which can make the interface bearing capacity more uniform and the coating is not easy to peel off. Based on the above analysis, the synergistic effect of cardanol epoxy monomer and GO can effectively enhance the tribological properties of epoxy composite coatings.

4. Conclusions

In this work, a bio-based epoxy resin with tertiary amine groups is synthesized through the green reaction of diethanolamine and cardanol epoxy resin, and was used to functionalize GO through simple electrostatic interaction to obtain bio-based graphene oxide (GOND) with reactive epoxy ends. It has been proven that this novel cardanol containing GO has facile dispersibility in epoxy matrix to afford the corresponding composite with excellent mechanical and tribological properties. Compared with pure epoxy resin, the epoxy nanocomposite material mixed with 0.5 wt% GOND has good storage modulus, elasticity and thermal stability, and the optimal addition content is 0.5%. In addition, the dry tribological test at room temperature showed that EP/GOND$_{0.5\%}$ also has the best wear resistance, which shows that GOND is beneficial to reduce the friction coefficient and wear rate of epoxy composites. The main reason for the above results is that the reactive bio-based epoxy grafted on the graphene oxide can enhance the interface interaction between the filler and the epoxy matrix; the GO nanosheets with good dispersion hinder the generation of cracks between the epoxy matrix and expand, and promote the load transfer efficiency between the filler and epoxy. Therefore, it can be considered that the synergistic effect of NC-514-DEA and GO makes the epoxy composite material have good mechanical properties and excellent tribological properties. The preparation procedure of this work is green, simple and effective, providing an effective method for the development of graphene-based epoxy composites with a wide range of applications.

Conflicts of interest

The authors declare no competing financial interest.

Acknowledgements

The authors are grateful for the financial support of the "One hundred Talented People" of the Chinese Academy of Sciences (No. Y60707WR04), the National Science Fund for Distinguished Young Scholars of China (No. 51825505) and the Key Research Projects of Frontier Science, Chinese Academy of Sciences (QYZDY-SSW-JSC009).

References

1 S. Pruksawan, S. Samitsu, Y. Fujii, N. Torikai and M. Naito, *ACS Appl. Polym. Mater.*, 2020, **2**, 1234–1243.
2 B. Xiao, M. Chen, R. Hu, X. Xu, X. Deng, Y. Niu, X. Li and H. Wang, *Adv. Eng. Mater.*, 2019, **21**, 1900981.
3 C. Liu, H. Zhao, P. Hou, B. Qian, X. Wang, C. Guo and L. Wang, *ACS Appl. Mater. Interfaces*, 2018, **10**, 36229–36239.
4 B. Zhao and T. Bai, *Carbon*, 2019, **144**, 481–491.
5 X. Zhao, W. Chen, X. Han, Y. Zhao and S. Du, *Compos. Sci. Technol.*, 2020, **191**, 108094.
6 Y. He, D. Wu, M. Zhou, H. Liu, L. Zhang, Q. Chen, B. Yao, D. Yao, D. Jiang, C. Liu and Z. Guo, *Appl. Surf. Sci.*, 2020, **506**, 144946.
7 O. Zabihi, H. Khayyam, B. L. Fox and M. Naebe, *New J. Chem.*, 2015, **39**, 2269–2278.
8 Y. He, Q. Chen, S. Yang, C. Lu, M. Feng, Y. Jiang, G. Cao, J. Zhang and C. Liu, *Composites, Part A*, 2018, **108**, 12–22.
9 H. Zhou, H. Wang, X. Du, Y. Mo, H. Yuan and H.-Y. Liu, *Composites, Part A*, 2019, **123**, 270–277.
10 M. Saha, P. Tambe and S. Pal, *Compos. Interfaces*, 2016, **23**, 255–272.
11 J. Peng, C. Huang, C. Cao, E. Saiz, Y. Du, S. Dou, A. P. Tomsia, H. D. Wagner, L. Jiang and Q. Cheng, *Matter*, 2020, **2**, 220–232.
12 V. Kumar, S. K. Sinha and A. K. Agarwal, *Tribol. Int.*, 2018, **127**, 10–23.
13 L.-C. Tang, Y.-J. Wan, D. Yan, Y.-B. Pei, L. Zhao, Y.-B. Li, L.-B. Wu, J.-X. Jiang and G.-Q. Lai, *Carbon*, 2013, **60**, 16–27.
14 J. Wei, M. S. Saharudin, T. Vo and F. Inam, *J. Reinf. Plast. Compos.*, 2018, **37**, 960–967.
15 Y.-J. Wan, L.-C. Tang, D. Yan, L. Zhao, Y.-B. Li, L.-B. Wu, J.-X. Jiang and G.-Q. Lai, *Compos. Sci. Technol.*, 2013, **82**, 60–68.
16 V. Palermo, I. A. Kinloch, S. Ligi and N. M. Pugno, *Adv. Mater.*, 2016, **28**, 6232–6238.
17 W. Xia, H. Xue, J. Wang, T. Wang, L. Song, H. Guo, X. Fan, H. Gong and J. He, *Carbon*, 2016, **101**, 315–323.

18 Y.-J. Wan, L.-C. Tang, L.-X. Gong, D. Yan, Y.-B. Li, L.-B. Wu, J.-X. Jiang and G.-Q. Lai, *Carbon*, 2014, **69**, 467–480.
19 M. C. Hsiao, S. H. Liao, M. Y. Yen, P. I. Liu, N. W. Pu, C. A. Wang and C. C. Ma, *ACS Appl. Mater. Interfaces*, 2010, **2**, 3092–3099.
20 L. Cao, X. Liu, H. Na, Y. Wu, W. Zheng and J. Zhu, *J. Mater. Chem. A*, 2013, **1**, 5081.
21 D. A. Bellido-Aguilar, S. Zheng, Y. Huang, X. Zeng, Q. Zhang and Z. Chen, *ACS Sustainable Chem. Eng.*, 2019, **7**, 19131–19141.
22 M. Natarajan and S. C. Murugavel, *J. Therm. Anal. Calorim.*, 2016, **125**, 387–396.
23 X. Wang, S. Zhou, W.-W. Guo, P.-L. Wang, W. Xing, L. Song and Y. Hu, *ACS Sustainable Chem. Eng.*, 2017, **5**, 3409–3416.
24 S. K. Sahoo, V. Khandelwal and G. Manik, *Polym. Adv. Technol.*, 2018, **29**, 565–574.
25 Y. Hu, Y. Wang, Z. Zeng, H. Zhao, X. Ge, K. Wang, L. Wang and Q. Xue, *Carbon*, 2018, **137**, 41–48.
26 C. Liu, J. Li, Z. Jin, P. Hou, H. Zhao and L. Wang, *Composites Communications*, 2019, **15**, 155–161.
27 S. Kanehashi, K. Yokoyama, R. Masuda, T. Kidesaki, K. Nagai and T. Miyakoshi, *J. Appl. Polym. Sci.*, 2013, **130**, 2468–2478.
28 L. G. Cancado, A. Jorio, E. H. Ferreira, F. Stavale, C. A. Achete, R. B. Capaz, M. V. Moutinho, A. Lombardo, T. S. Kulmala and A. C. Ferrari, *Nano Lett.*, 2011, **11**, 3190–3196.
29 C. Liu, P. Du, H. Zhao and L. Wang, *ACS Appl. Nano Mater.*, 2018, **1**, 1385–1395.
30 M. Peng, X. Tang and Y. Zhou, *Polymer*, 2016, **93**, 1–8.
31 X. Tang, Y. Zhou and M. Peng, *ACS Appl. Mater. Interfaces*, 2016, **8**, 1854–1866.
32 X. Zhu, Q. Yan, L. Cheng, H. Wu, H. Zhao and L. Wang, *Chem. Eng. J.*, 2020, **389**, 124435.
33 M. A. Rafiee, J. Rafiee, I. Srivastava, Z. Wang, H. Song, Z. Z. Yu and N. Koratkar, *Small*, 2010, **6**, 179–183.
34 J. Li, W. Zhu, S. Zhang, Q. Gao, J. Li and W. Zhang, *Polym. Test.*, 2019, **76**, 232–244.
35 J. Yang, C. Shao and L. Meng, *Langmuir*, 2019, **35**, 10542–10550.
36 L.-Z. Guan, Y.-J. Wan, L.-X. Gong, D. Yan, L.-C. Tang, L.-B. Wu, J.-X. Jiang and G.-Q. Lai, *J. Mater. Chem. A*, 2014, **2**, 15058.
37 S. Wan and Q. Cheng, *Adv. Funct. Mater.*, 2017, **27**, 1703459.
38 P. Li, Y. Zheng, T. Shi, Y. Wang, M. Li, C. Chen and J. Zhang, *Carbon*, 2016, **96**, 40–48.
39 R. K. Upadhyay and A. Kumar, *Tribol. Int.*, 2019, **130**, 106–118.
40 C. Chen, S. Qiu, M. Cui, S. Qin, G. Yan, H. Zhao, L. Wang and Q. Xue, *Carbon*, 2017, **114**, 356–366.

